Astron. Astrophys. 338, 311–321 (1998)

ASTRONOMY AND ASTROPHYSICS

On the generation of nonlinear magnetic tube waves in the solar atmosphere

II. Longitudinal tube waves

P. Ulmschneider[1] **and Z.E. Musielak**[2,1]

[1] Institut für Theoretische Astrophysik der Universität Heidelberg, Tiergartenstrasse 15, D-69121 Heidelberg, Germany
[2] Center for Space Plasma, Aeronomy, and Astrophysics Research, University of Alabama, Huntsville, AL 35899, USA

Received 13 March 1998 / Accepted 22 June 1998

Abstract. The nonlinear time-dependent response to external pressure fluctuations acting on a thin vertical magnetic flux tube embedded in the solar atmosphere is investigated numerically. The continuous and impulsive fluctuations are imposed on the tube at different atmospheric heights and the resulting longitudinal tube wave energy fluxes are calculated for an observationally established range of velocity amplitudes and tube magnetic fields. The obtained results show that typical wave energy fluxes carried by nonlinear longitudinal tube waves are of the order of $2 \cdot 10^8\ erg/cm^2s$, which is roughly a factor of 30 less than the flux for transverse waves. In contrast to our linear analytical results the generated nonlinear longitudinal tube wave fluxes can be up to an order of magnitude higher.

Key words: waves – MHD – methods: numerical – Sun: chromosphere – Sun: corona – Sun: magnetic fields

1. Introduction

In this second of a series of papers we continue our study of the generation of different types of nonlinear magnetic tube waves in the solar atmosphere. In the first paper, see Huang et al. (1995, henceforth called Paper I), we have investigated the generation of nonlinear transverse tube waves by shaking a thin magnetic flux tube with velocity perturbations of an observed magnitude which vary according to an inferred spectrum of the solar turbulent convection. In the present paper, we apply external pressure perturbations to the tube and calculate the efficiency of generation of nonlinear longitudinal tube waves. Our approach is fully numerical and is, therefore, different from other previous (mostly analytical) treatments of the generation of magnetic tube waves (e.g., Musielak et al. 1989; Choudhuri et al. 1993a, 1993b; Musielak et al. 1995). In the work by Musielak et al. (1995), a general theory of interaction of magnetic flux tubes with the subsonic turbulent convection has been developed and used to investigate the generation of linear longitudinal and transverse tube waves. The obtained results show that the fluxes can be important for the heating observed in the solar chromospheric network and that they should be regarded only as lower bounds for realistic energy fluxes carried by these waves. Choudhuri et al. have investigated the generation of magnetic kink waves by rapid foot point motions of the magnetic flux tube. They argue that occasional rapid motions can account for the entire energy flux needed to heat the quiet corona. They find that pulses are much more efficient than continuous excitation for the transfer of wave energy to the solar corona and that the energy flux from pulses actually increases if there is a transition layer temperature jump in the atmosphere.

The approach presented by us in Paper I and in this paper can be justified by recent observations of the proper motions of footpoints of magnetic flux tubes at the photospheric level (Muller 1989; Nesis et al. 1992; Muller et al. 1994) and by time-dependent numerical simulations of the solar convection (e.g., Nordlund & Dravins 1990; Nordlund & Stein 1991; Cattaneo et al. 1991; Steffen 1993). Both the observations and numerical simulations clearly show that horizontal velocities as large as 3 km/s occur in the solar photosphere and at the top of the convection zone. Velocities of this magnitude and larger have also been seen by Title (1994, private communication) in his observational data. In addition, in some of these numerical simulations evidence has been found for the presence of horizontally propagating shock waves (Cattaneo et al. 1991; Steffen 1993, Solanki et al. 1996a, Steiner et al. 1996, 1998). The existence of granular transsonic flows has also been reported by Nesis et al. who interpreted some of their data as post-shock turbulence; this interpretation has been criticized by Solanki et al. who claim that there is no conclusive evidence for these flows in the Nesis et al. data but there is a signature of shocks in their data. Recently, Nordlund et al. (1997) have suggested that the granulation flow is seemingly laminar despite of the high Reynolds numbers involved and that the level of turbulence in this flow is much lower than previously assumed. Based on these contradictory results, it is clear that the problem of the existence of granular supersonic flows and post-shock turbulence is far from being solved despite the concentrated observational and theoretical efforts. Without going further into details of this dis-

Send offprint requests to: P. Ulmschneider
Correspondence to: ulmschneider@ita.uni-heidelberg.de

cussion, we restrict our calculations to subsonic motions (see Sect. 2) and investigate numerically the interaction of these motions with magnetic flux tubes. The fact that this interaction may become an efficient source of magnetic tube waves which can propagate along the tubes and carry energy to the chromosphere and corona has already been recognized in the literature (see Narain & Ulmschneider 1996, and references therein). A rough estimate of the generated wave energy fluxes by Muller et al. (1994) clearly demonstrates that the amount of wave energy available for heating is sufficient to sustain the mean level of the observed radiative losses from both the solar chromosphere and corona.

The aim of the present paper is to calculate the wave energy fluxes generated by the interaction between a thin magnetic flux tube and the pressure fluctuations produced by turbulence in the solar photosphere and convection zone. We consider the continuous excitation of nonlinear longitudinal tube waves by these fluctuations and assume that the fluctuations are symmetric and are caused by the turbulent flow field. The fact that the imposed perturbations on a thin, vertically oriented magnetic flux tube are symmetric, results in a symmetric squeezing of the tube and in the excitation of *purely* longitudinal tube waves. Note that in this process the tube is not displaced from its vertical position.

This generation of longitudinal tube waves distinguishes the results of the present paper from those obtained in Paper I. Note that in Paper I, the excited nonlinear transverse tube waves were always coupled to longitudinal tube waves via the process of nonlinear mode coupling. As shown by Ulmschneider et al. (1991), the coupling can be an important way to dissipate the energy carried by the generated nonlinear transverse tube waves (Zhugzhda et al. 1995). In our present work, however, the excitation of nonlinear longitudinal tube waves is direct and a much more efficient shock dissipation will result in the chromospheric flux tube (Herbold et al. 1985).

In order to prescribe the external pressure fluctuations imposed on the tube, we specify the rms velocity amplitude of the external turbulent motions and use an extended Kolmogorov spectrum with a modified Gaussian frequency factor (Musielak et al. 1994). Note that the basic procedure for determining the fluctuations is similar to that presented in Paper I. The horizontal pressure balance translates the external pressure fluctuations into internal pressure and magnetic field fluctuations. Using the linear relations between longitudinal velocity-, pressure- and magnetic field perturbations, valid for small amplitude longitudinal tube waves, the fluctuations can be described by internal velocity perturbations alone which serve as piston boundary condition for the generated longitudinal tube wave.

To prescribe the external pressure perturbations by using a turbulent energy spectrum has another advantage. The representation of the perturbation spectrum by a large number of partial waves occasionally results in large wave amplitudes which are precisely those events which Choudhuri et al. envision to produce the bulk of the wave energy. We will show below (c.f. Fig. 4) that the longitudinal wave flux generation (like the transverse wave generation in Paper I) indeed displays this behaviour. Our approach to use realistic turbulent energy spectra thus permits to accurately describe the stochastic wave generation process.

The main numerical tool used in this paper is a one-dimensional, time-dependent, nonlinear MHD code originally developed by Herbold et al. (1985) to study the vertical propagation of longitudinal waves in thin magnetic flux tubes. A modified version of this code by Ulmschneider et al. (1991) has been used to study the propagation of longitudinal-transverse magnetic tube waves as well as the transverse wave generation in Paper I. Note that the use of the transverse equation of motion adopted from Spruit (1981) in the Ulmschneider et al. (1991) code has been criticized by a considerable number of authors (for details and the literature see Cheng 1992; Moreno-Insertis et al. 1997). These criticisms apply only to the back reaction force experienced by the tube upon swaying, but do not have any bearing on our present problem which does not allow for swaying. In addition, as shown by Osin et al. (1998), due to the lack of sizeable longitudinal flows, these criticisms do not appreciably influence the case of the transverse tube wave energy generation of Paper I or the wave propagation results of Ulmschneider et al. (1991). For our present calculation the transverse equation of motion was disregarded and the Herbold et al. code, which considers only the longitudinal equation of motion, was modified to perform our calculations of the excitation of nonlinear longitudinal tube waves.

We organize the paper as follows: Sect. 2 describes briefly the basic assumptions and the method; the results of our calculations are presented in Sect. 3, and finally Sect. 4 gives our conclusions.

2. Basic assumptions and the method

2.1. Tube model

We consider a thin, vertically oriented magnetic flux tube embedded in the solar atmosphere and excite nonlinear longitudinal tube waves by squeezing the tube symmetrically at different heights. We assume that the external pressure perturbations caused by the photospheric and subphotospheric turbulent motions are responsible for the squeezing and that these perturbations can be represented by a superposition of partial waves with random phases derived from the local turbulent flow field. The maximum rms velocity of the turbulent motions is taken from a range of observed velocities on the solar surface (e.g., Muller 1989; Nesis et al. 1992; Muller et al. 1994) as well as from numerical simulations of turbulent convection (e.g., Cattaneo et al. 1991; Steffen 1993). For the magnetic tube model, we assume that in the solar atmosphere described by model C of Vernazza et al. (1981) a vertically oriented flux tube is embedded and that the tube has a radius of $50\ km$ and a field strength of $B_0 = 1500\ G$ at the height where externally the optical depth is $\tau_{5000} = 1$. This field strength appears to be typical for magnetic flux tubes residing in the supergranular boundaries; for recent direct measurements of these fields see Solanki et al. (1996b). To show the dependence on the field strength we also consider tubes with $B_0 = 1000$ and $1250\ G$. The tubes are

assumed to spread exponentially with height in accordance to horizontal pressure balance and magnetic flux conservation. As the maximum of the convective velocities both in mixing-length models and in numerical convection zone models occur deeper than $\tau_{5000} = 1$, we select excitation heights at $\tau_{5000} = 1$, 10 and 100 in optical depth measured outside the tube. Because the Vernazza et al. model goes only to $\tau_{5000} \approx 10$, we extended that model by fitting a convection zone model obtained with the code of Bohn (1981, 1984).

2.2. Pressure balance

To calculate wave energy spectra and fluxes carried by nonlinear longitudinal tube waves, we must prescribe external pressure fluctuations which lead to symmetrical squeezing of the tube. As discussed earlier, the perturbations are caused by the turbulent motions of the external medium. Therefore, in order to prescribe the perturbations we have to know the physical properties of the turbulence. Unfortunately, the properties of realistic turbulence occuring on the Sun are presently unknown and currently no first principle theory of turbulence exists. Therefore, the properties of the turbulence occuring on and below the solar surface are usually determined by specifying a turbulent energy spectrum. Many different shapes of the turbulent energy spectrum in the solar atmosphere have been proposed (e.g, Stein 1967; Bohn 1984; Musielak et al. 1989; Goldreich & Kumar 1988, 1990). More recently, Musielak et al. (1994) have combined some theoretical arguments about the turbulence with the results of numerical simulations (e.g., Cattaneo et al. 1991) as well as observational results (e.g., Zahn 1987; Muller et al. 1994) and suggested that the spatial and temporal parts of the turbulent energy spectrum can be described by an extended Kolmogorov spectrum with a modified Gaussian frequency factor. Recently, Nordlund et al. (1997) have argued that the Kolmogorov scaling with a power spectrum slope of $-5/3$ may not apply in regions of highly non-isotropic motions found in convection zone simulations. They also argue that the turbulence is reduced in rising bulk flows and enhanced in downflows. This could increase our tube wave generation rates as the magnetic tubes are indeed situated in the downflow regions. In addition it has to be noted that bulk downflows along and outside the magnetic flux tubes do not contribute to the wave generation. For the superposed isotropic velocity fluctuations which we envision at our shaking point, we expect on basis of the high Reynolds numbers, that the Kolmogorov spectrum is well represented, particularly as the tube excitation is at large optical depths (at the point of the maximum of the convective velocity at $\tau \approx 10$ to 100), where radiation effects are still minor. For the range of this spectrum we feel that it would be hard to deviate greatly from the typical length scale in a gravitational atmosphere, the scale height H, and the subsequent inertial breakup cascade to sizes as small as $H/100$.

Following Musielak et al. (1995) we write the pressure balance between the tube and the external medium as

$$p + \frac{B^2}{8\pi} = p_e + p_{turb} \quad , \tag{1}$$

where p is the internal gas pressure, B the magnetic field strength in the tube, p_e the external gas pressure and

$$p_{turb} = \rho_e \left(v_x^2(\mathbf{r},t) + v_y^2(\mathbf{r},t) + v_z^2(\mathbf{r},t) \right) \quad , \tag{2}$$

is the time-dependent external turbulent pressure. v_x, v_y, v_z are the turbulent velocities in x, y, z-directions which are functions of position $\mathbf{r}$ and time t. Upon time averaging one gets

$$u_{xt} = \sqrt{\overline{v_x(\mathbf{r},t)^2}},\ u_{yt} = \sqrt{\overline{v_y(\mathbf{r},t)^2}},\ u_{zt} = \sqrt{\overline{v_z(\mathbf{r},t)^2}} \quad . \tag{3}$$

For the case of homogeneous isotropic turbulence there is no longer a dependence on $\mathbf{r}$ due to the assumed homogeneity and for the three spatial components one has

$$u_t = u_{xt} = u_{yt} = u_{zt} \quad , \tag{4}$$

because of the assumed isotropy. Here u_t is the rms velocity amplitude in one spatial direction, taken to be the same in the x, y and z-directions, it is independent of space and time. Note that our present definition of u_t agrees with the notation in Paper I, and with that used in Eqs. (B6), (B10) and (18) of Musielak et al. (1995), while unfortunately the same notation u_t was also used in a different sense in Eqs. (2), (6) and (8) of the latter paper to describe the total time-dependent 3-D turbulent velocity vector. From the above equations we find for the time-averaged external turbulent pressure

$$\overline{p_{turb}} = 3\rho_e u_t^2 \quad . \tag{5}$$

After time-averaging of Eq. (1) and assuming homogeneous isotropic turbulence we obtain

$$p_0 + \frac{B_0^2}{8\pi} = p_e + 3\rho_e u_t^2 \quad , \tag{6}$$

where p_0 is the average internal gas pressure and B_0 the average magnetic field strength. This equation shows that when one adds a turbulent flow outside the magnetic flux tube, then the mean external pressure is increased. This is due to the fact that in Eqs. (1), (2) the external turbulent pressure is a quantity which cannot be negative and thus must fluctuate around an average positive value. Typically the mean turbulent pressure leads to a small additional compression of the flux tube relative to the static case. With $p_e = 1.7 \cdot 10^5\ dyn/cm^2$, $\rho_e = 3.3 \cdot 10^{-7}\ g/cm^3$ and $u_t = 1\ km/s$, we find $\overline{p_{turb}} = 5.8 \cdot 10^{-2} p_e$. Note that because of this, $\overline{p_{turb}}$ has been neglected relative to p_e in the paper of Musielak et al. (1995) in their analytical treatment of the generation of linear longitudinal tube waves.

As we are interested in the fluctuating quantities we subtract Eq. (6) from (1) and upon linearization obtain

$$p' + \frac{B_0 B'}{4\pi} = p_{turb} - 3\rho_e u_t^2 = p'_{turb} \quad , \tag{7}$$

where $p' = p - p_0$ is the internal gas pressure perturbation and $B' = B - B_0$ the magnetic field strength perturbation.

2.3. Turbulent velocity fluctuations

Following Paper I we assume that the horizontal turbulent velocity fluctuations in the x-direction can be represented by a linear combination of N = 100 partial waves

$$v_x(t) = \sum_{n=1}^{N} u_n \sin(\omega_n t + \varphi_n) \quad , \tag{8}$$

where u_n is the velocity amplitude of these waves, it will be determined by the turbulent energy spectrum (see below), ω_n is the wave frequency that ranges from 2.9 to 290 mHz with step $\Delta\omega_n = 2.9$ mHz, and $\varphi_n = 2\pi r_n$ is an arbitrary but constant phase angle with r_n being a random number in the interval [0, 1]. Note that these limits correspond to $\omega_A/10$ and $10\ \omega_A$, where $\omega_A = 2\pi/P_A = c_S/(2H)$ is the acoustic cut-off frequency. Note also that the right hand side (RHS) of Eq. (8) cannot be formally treated as a Fourier decomposition of $v_x(t)$ in time because of the random phases φ_n of the otherwise sinusoidal waves.

To determine the velocity amplitudes u_n, we follow the procedure outlined in Paper I. We begin with time averaging v_x^2 to find

$$\overline{v_x^2} = \frac{1}{2}\sum_{n=1}^{N} u_n^2 \quad , \tag{9}$$

from which using Eqs. (3) and (4) we have

$$u_t^2 = \frac{1}{2}\sum_{n=1}^{N} u_n^2 \quad . \tag{10}$$

As described in Paper I as well as by Musielak et al. (1995) the turbulent energy spectrum is normalized to

$$\frac{3}{2}u_t^2 = \int_0^\infty d\omega \int_0^\infty dk\ E(k) G\left(\frac{\omega}{ku_k}\right) = \int_0^\infty E'(\omega) d\omega \quad , \tag{11}$$

where $E(k)$ and $G(\omega/ku_k)$ are the spatial and temporal components of the turbulent energy spectrum, respectively. Here the factor $3/2$ results from the contributions to the kinetic energy from the three spatial directions. We now use Eq. (10) to write u_t as

$$\frac{3}{2}u_t^2 = \frac{3}{4}\sum_{n=1}^{N} u_n^2 = \int_0^\infty E'(\omega) d\omega = \sum_{n=1}^{N} E'(\omega_n)\Delta\omega \quad , \tag{12}$$

from which we have

$$u_n = \sqrt{\frac{4}{3}E'(\omega_n)\Delta\omega} \quad , \tag{13}$$

with

$$E'(\omega_n) = \int_0^\infty E(k) G\left(\frac{\omega_n}{ku_k}\right) dk \quad . \tag{14}$$

Comparing our present Eqs. (12), (13) with Eqs. (25), (26) of Paper I we notice an error in Paper I which leads to an underestimate of the transverse tube wave fluxes of that paper by a factor of 2. As mentioned in Paper I, the combined shaking by a horizontal velocity similar to $v_H = \sqrt{v_x^2 + v_y^2}$ could increase the transverse flux even more, but depends on correlation effects. As we assume that the shaking in x and y-directions are uncorrelated, the total transverse wave flux by shaking with v_x and v_y is a factor of two higher than that found when shaking with v_x alone. Thus compared to the values given in Table 1 of Paper I, the true total transverse wave fluxes should be a factor of 2-4 higher. That is, the transverse wave flux should be of the order of $6.0 \cdot 10^9\ erg\ cm^{-2}s^{-1}$. Note that contrary to the longitudinal wave case, the fluctuations v_z do not contribute to the transverse wave flux.

To specify the turbulent energy spectra appropriate for the solar convection zone we follow Musielak et al. (1994). These authors argue on the basis of observations and numerical simulations of the solar convection that a realistic turbulent energy spectrum should be reasonably well described by an extended Kolmogorov spectrum $E(k)$ and a modified Gaussian frequency factor $G(\frac{\omega}{ku_k})$. The extended Kolmogorov spatial spectrum is given by

$$E(k) = \begin{cases} 0 & 0 < k < 0.2k_t \\ a\frac{u_t^2}{k_t}\left(\frac{k}{k_t}\right) & 0.2k_t \le k < k_t \\ a\frac{u_t^2}{k_t}\left(\frac{k}{k_t}\right)^{-5/3} & k_t \le k \le k_d \end{cases} \quad , \tag{15}$$

where the factor $a = 0.758$ is determined by the normalization condition

$$\int_0^\infty E(k)dk = \frac{3}{2}u_t^2 \quad , \tag{16}$$

and $k_t = 2\pi/H$, where H is the scale height. k_d is the wave number where the turbulent cascade ends, for which Theurer et al. (1997) have estimated values as high as $k_d = 2\pi/L$ where $L \approx 2.9\,cm$, for our purposes it is sufficient to take $L = H/100$. The modified Gaussian frequency factor is described by

$$G\left(\frac{\omega}{ku_k}\right) = \frac{4}{\sqrt{\pi}}\frac{\omega^2}{|ku_k|^3}e^{-(\frac{\omega}{ku_k})^2} \quad , \tag{17}$$

where u_k is computed from

$$u_k = \left[\int_k^{2k} E(k')dk'\right]^{1/2} \quad . \tag{18}$$

Knowing $E(k)$ and $G(\omega/ku_k)$, we may now use Eqs. (13), (14) to calculate the velocity amplitude u_n of the partial waves. The resulting amplitudes u_n obtained in this way are shown in Fig. 1.

The results presented in Fig. 1 can now be used to compute the turbulent velocity fluctuations $v_x(z_{sh}, t)$ at the squeezing height z_{sh} using Eq. (8). Fig. 2 shows v_x (dashed) at the squeezing height $z_{sh}(\tau = 10)$ as a function of time t up to $t = 5000\ s$. This corresponds to $t = 25P_A$. It is seen that due to the many

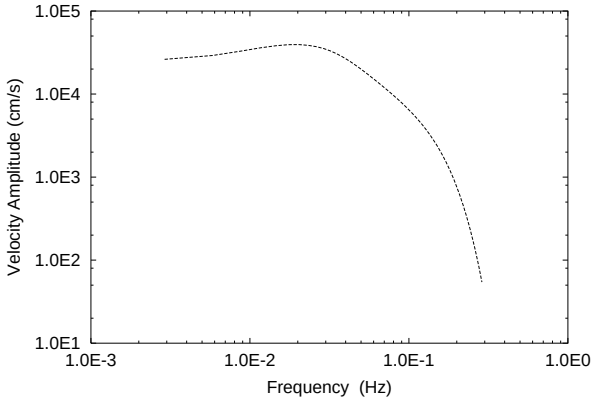

Fig. 1. The velocity amplitude u_n for each partial wave of the frequency ω_n, computed using Eq. (13) for a prescribed rms turbulent velocity of $u_t = 1\ km/s$.

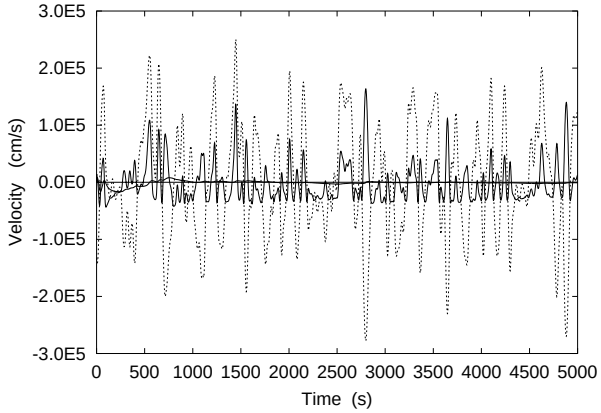

Fig. 2. Horizontal fluctuating turbulent velocity v_x (dashed) computed from Eq. (8) as well as the internal longitudinal velocity $v_\parallel$ (solid) computed from Eq. (24) for the velocity amplitudes given in Fig. 1. Also shown are the zero velocity line (thin solid) and the time average $\overline{v_\parallel}$ (solid) which from times $t > 1000\ s$ is essentially identical to the zero velocity line (which it should be).

partial waves with random phases, v_x is very stochastic in nature. Since the RHS of Eq. (8) does not represent a Fourier decomposition of $v_x(t)$ in time, and since $v_x(t)$ can be treated as a non-periodic signal restricted in time to $0 \leq t \leq 5000$ s, we may now perform Fourier analysis of this signal by calculating its Fourier transform, $\mathcal{F}v_x(t) = v_x(\omega)$, and the corresponding power spectrum, $P_v(\omega) = |v_x(\omega)|^2$. To normalize $P_v(\omega)$, we compute

$$P_{tot} = \int_0^\infty P_v(\omega) d\omega \quad , \tag{19}$$

and introduce the normalized power spectrum of the turbulent velocity $v_x(t)$ by defining $v_{xs}(\omega) = u_t P_v(\omega)/P_{tot}$; in the following we call v_{xs} simply the velocity spectrum. This spectrum has dimension of $cm\ s^{-1}\ Hz^{-1}$ and is plotted in Fig. 3. The presented spectrum was obtained from temporal Fourier analysis of the last 2048 s of the velocity $v_x(t)$, where the velocity was sampled every sec. The lower limit of the spectrum is due to the total sampling time. As seen in Fig. 3, the velocity spectrum shows no discrete lines for any frequency but only broad noise which indicates completely aperiodic (chaotic) motions. This confirms that the velocity field described by Eq. (8) is indeed chaotic in nature as should be expected for the turbulent velocity fluctuations.

2.4. Fluctuating turbulent pressure

In the process of the longitudinal tube wave excitation the tube is compressed symmetrically by the external turbulent pressure. This turbulent pressure consists of a time averaged term $\overline{p_{turb}}$ which augments the external gas pressure p_e and a fluctuating term which gives rise to longitudinal tube waves. Assuming isotropic homogeneous turbulence, the fluctuating turbulent pressure (see Eq. 7) is given by

$$p'_{turb} = \rho_e \left(v_x^2 + v_y^2 + v_z^2\right) - 3\rho_e u_t^2 \approx 3\rho_e (v_x^2 - u_t^2) \quad . \tag{20}$$

Here after Eq. (2) we should have used uncorrelated values of v_x^2, v_y^2 and v_z^2, but as the spectrum already consists of a large number of independent partial waves, the excitation with independent v_y and v_z will not bring anything new. Combining Eqs. (7) and (20), one sees that the external pressure fluctuations are translated into pressure and magnetic field fluctuations inside the tube.

As our Lagrangian wave code uses a velocity boundary condition, we make use of the amplitude relations for longitudinal tube waves (Herbold et al. 1985, Eq. 59) to translate the gas pressure fluctuations into internal longitudinal velocity fluctuations

$$v_\parallel = \frac{c_S^2}{c_T} \frac{p'}{\gamma p_0} \quad , \tag{21}$$

where c_S is the sound speed, $c_T = (1/c_S^2 + 1/c_A^2)^{-1/2}$ the tube speed, c_A is the Alfvén speed and γ is the ratio of specific heats.

Note at this point that the amplitude relation of Eq. (21), like relations for pure acoustic waves, is only valid for frequencies large compared to the cut-off frequency for longitudinal tube waves; this frequency was first introduced by Defouw (1976; see also Roberts & Webb 1979). For wave frequencies close to this cut-off, phase-shifts between p' and $v_\parallel$ enter Eq. (21), which approach 90^0. However, as the Lagrangian code permits to specify only one physical quantity (the velocity $v_\parallel$) as boundary condition we are not affected by this phase-shift. Note that in an explicit time-dependent Lagrangian wave code the three unknowns (velocity and two thermodynamic variables) are exactly determined by the relations along the three characteristics (C^+, C^-, C^0). At the top and bottom boundaries one characteristic is missing and is replaced by boundary conditions while the other two unknowns (e.g. p' and S) are determined by relations along the remaining two characteristics (e.g. C^- and the fluid path C^0) by which the phase-shift is automatically computed and taken into account. This is particularly gratifying as for an acoustic wave spectrum (as opposed to a monochromatic wave)

the influence of the phase-shift would be difficult to determine analytically.

The remaining problem is now to connect in Eq. (7) the internal gas pressure fluctuation p' with the external turbulent pressure fluctuation p'_{turb}. Here we follow Hasan (1997). Neglecting gravity and assuming that the squeezing of the tube occurs over a considerable height span (that is, taking his $d\xi_z/dz = 0$) we find from his Eq. (35)

$$\frac{p'}{p_0} = \frac{\gamma(\beta+1)}{2+\gamma\beta}\frac{p'_e}{p_e} \tag{22}$$

from which, as p'_e is our p'_{turb}, we derive

$$p' = \frac{\beta}{2/\gamma+\beta}p'_{turb} \quad . \tag{23}$$

Here $\beta = 8\pi p_0/B_0^2$ is the plasma β. Note that for $\beta \to \infty$, that is, when the magnetic field vanishes, this relation goes to the correct limit $p' = p'_e$ while for $\beta \to 0$, when the tube becomes entirely empty of gas, ($p_0 = 0$), the expected limit $p' = 0$ is reached. Note in passing that Eqs. (21) and (22) valid for longitudinal tube waves are very similar to the familiar amplitude relations $v/c_S = p'/(\gamma p_0) = \rho'\rho_0$ of pure sound waves. Finally Eqs. (20), (23) allow to write Eq. (21) as

$$v_\parallel = \frac{\beta}{2/\gamma+\beta}\frac{p'_{turb}}{\rho_0 c_T} = \frac{\beta}{2/\gamma+\beta}\frac{3\rho_e(v_x^2-u_t^2)}{\rho_0 c_T} \quad . \tag{24}$$

Fig. 2 shows (solid) the internal longitudinal velocity $v_\parallel$ which corresponds to the applied external velocity v_x displayed in the same figure. The close relationship of the two velocities is apparent. While v_x obviously oscillates around zero (see Fig. 2), $v_\parallel$ is clearly very one-sided. However, as $\overline{v_x^2} = u_t^2$, the time-average of $v_\parallel$ must also be zero. To check the oscillatory character of $v_\parallel$, we calculated $\overline{v_\parallel}$=$\int v_\parallel\, dt/\int dt$ ($\overline{v_\parallel}$ is shown solid in Fig. 2) and found that $v_\parallel$ indeed oscillates around zero. The oscillations of $v_\parallel$ are not symmetric because large absolute velocities $|v_x| >> u_t$ produce large turbulent pressure fluctuations $v_x^2 >> u_t^2$ and thus large positive velocity spikes $v_\parallel$, while small velocities $v_x \approx 0$ lead to small turbulent pressures and negative velocities $v_\parallel$. The negative velocity spikes are much smaller because, according to Eq. (24), they are at most proportional to $-u_t^2$.

2.5. Longitudinal wave energy fluxes

For the instantaneous longitudinal tube wave flux at height z we take (Herbold et al. 1985, Eq. (58), Hasan 1997, Eq. (32))

$$F(z,t) = v_\parallel(z,t)p'(z,t) \quad . \tag{25}$$

Since we want to compare wave energy fluxes generated at different heights in the tube it is appropriate to normalize the fluxes to the solar surface, that is, to the height $z = 0$, for which outside the tube we have $\tau_{5000} = 1$. At this height the tube radius has a cross-section $A_0 = A(z = 0)$, while at other heights it has

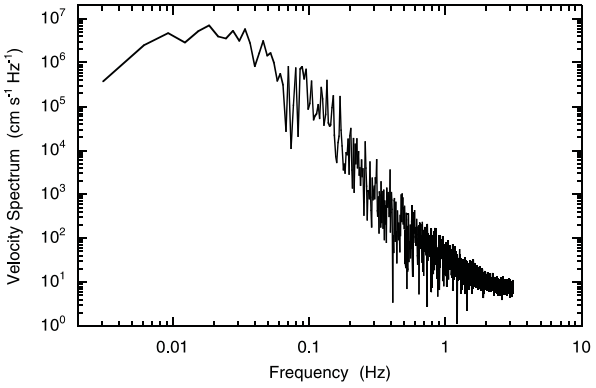

Fig. 3. Normalized power spectrum of the fluctuating turbulent velocity v_x shown in Fig. 2. This velocity spectrum is shown as a function of circular frequency ω.

the cross-section A. The normalized time-averaged flux with $A_0\overline{F(z=0)} = A(z)\overline{F(z)}$ can be written as

$$F_L = \overline{F(z=0)} = \frac{A(z)}{A_0}\overline{v_\parallel(z,t)p'(z,t)} \quad , \tag{26}$$

where as above the overline indicates time averaging. The wave energy spectrum is calculated by taking the Fourier transform of $F(z,t)$ by using the procedure outlined in Sect. 2.3.

The expressions (25), (26) for the longitudinal wave energy flux can be shown to be correct by introducing the wave solutions (Eqs. (A.1) to (A.6)) of Herbold et al. (1985) into the energy conservation equation for longitudinal tube waves (Hasan 1997, Eqs. (30) to (32)) from which the correct dispersion relation for these waves is recovered. We are very grateful to S. Hasan (1997, private communication) and Y. Zhugzhda (1998, private communication) for pointing out to us that the expression $F = (1+5\beta/4)v_\parallel p'$ for the longitudinal wave energy flux used in our previous papers (Musielak et al. 1989, 1995) is inappropriate, as it mixes a wave flux and a 'wave wind'. The total wave energy flux integrated over the tube cross-section is $\left(A_0\overline{\rho' v} + \rho_0\overline{A' v}\right) H_0 + A_0\overline{p' v}$ where H is the enthalpy. By convention (Landau & Lifshitz 1959, Sect. 64) the first two terms arising from the linearized version of the mass flux $A\rho v$ are usually not included in the wave flux. However, note that the additional term $(5\beta/4)v_\parallel p'$ used by Musielak et al. arises from the 'mass flux' term $\rho_0\overline{A' v}H_0$ and gives a contribution even when there is no net flow velocity $\overline{v}$, it thus will always be present in a wave. As in the Musielak et al. papers β was ≈ 0.3, the analytical longitudinal tube wave flux was overestimated by a factor of 1.38. Such a correction is small against the overall uncertainties in these type of calculations.

At this point we summarize the somewhat circuitous logic of the procedure to obtain the generated longitudinal wave flux. The external turbulent motions of the convection zone generate pressure fluctuations $p'_{turb}(z_{sh},t)$ (here z_{sh} is the squeezing height and t the time) which can be translated into internal gas pressure fluctuations $p'(z_{sh},t)$. As our time-dependent longitudinal wave code requires velocity fluctuations $v_\parallel(z_{sh},t)$ as boundary condition, we use the amplitude relations for longitu-

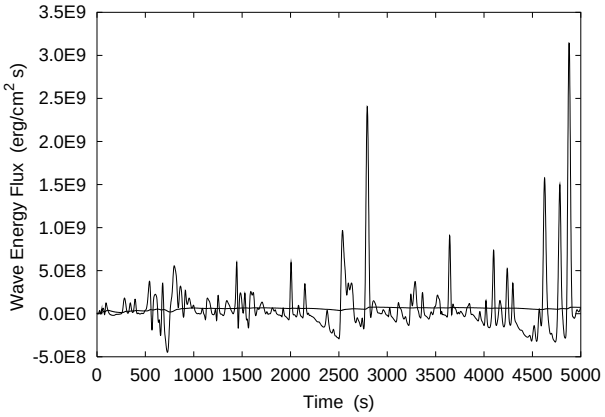

Fig. 4. Instantaneous and time-averaged longitudinal tube wave energy flux for a tube with $B = 1500\ G$ (case 3 of Table 1). The stochastic nature of the wave generation is shown.

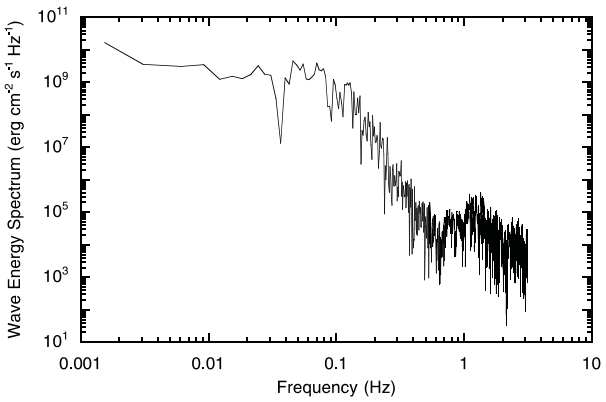

Fig. 5. Normalized power spectrum of the instantaneous wave energy flux presented in Fig. 4. This wave energy spectrum is shown as a function of circular frequency ω and its stochastic nature can again be clearly seen.

dinal tube waves to replace $p'(z_{sh},t)$ by $v_\parallel(z_{sh},t)$. One might think that, as we have $p'(z_{sh},t)$ and $v_\parallel(z_{sh},t)$, one could directly compute the longitudinal tube wave flux from Eq. (26) without using the wave code. This is wrong, as in such a product the phase-shift (time-delay) between the quantities would not be taken into account. For monochromatic waves this phase-shift is known, but not for a wave spectrum. In the wave code we take $v_\parallel(z_{sh},t)$ as boundary condition, which is applied somewhat time-delayed but has the correct magnitude. The wave code then self-consistently generates new gas pressure fluctuations $p'_{new}(z_{sh},t)$ which differ from the above mentioned p', but now have the correct phase shift against the velocity fluctuations $v_\parallel(z_{sh},t)$. The wave code thus ensures that the quantities $p'_{new}(z_{sh},t)$ and $v_\parallel(z_{sh},t)$ have the correct phase shift required for the wave flux determination in Eqs. (25) and (26).

3. Results and discussion

For specified rms turbulent velocities in the range of $u_t = 1$ to $1.5\ km/s$, squeezing at three different excitation heights z_{sh} (specified in terms of optical depths τ_{5000}= 1, 10, 100), we have computed time-averaged longitudinal wave energy fluxes F_L in magnetic flux tubes with field strengths $B_0 = 1000,\ 1250$ and $1500\ G$ where B_0 is specified at $\tau_{5000} = 1$. The tube was excited by specifying $v_\parallel(z_{sh},t)$, using Eq. (24), where the fluctuating horizontal flow field with velocity $v_x(z_{sh},t)$ is given by Eq. (8) and where $u_t^2 = \overline{v_x^2}$. The partial wave amplitudes u_n are computed from Eq. (13). This flow field is assumed to represent the isotropic turbulence acting as pressure fluctuations on the tube boundary.

The resulting normalized wave energy fluxes computed by using Eq. (26) for different cases of tube excitation are shown in Table 1. The results clearly demonstrate (see cases 10-13 or 14-17) that the fluxes depend strongly on the magnitude u_t of the external turbulent velocity perturbation. Eq. (26) and cases 7 to 9 show that there is also a significant dependence on B_0 in the sense that with larger B_0 one gets smaller fluxes F_L. This is due to the fact that a stronger tube becomes more rigid and thus less easily perturbed by outside pressure fluctuations. The numerically determined dependences on u_t and B_0 (at $\tau = 10$) can be roughly fitted by

$$F_L^* \approx 1.76 \cdot 10^{-3} u_t^{4.13} B_0^{-3.16} \quad , \tag{27}$$

with u_t in (cm/s) and B_0 in (G). The approximate values from this formula are also shown in Table 1. A similar dependence of the longitudinal wave flux has been found in the analytical calculations by Musielak et al. (1989, 1995).

Table 1 also shows that the wave fluxes do not depend much on the height of the excitation point (compare cases 1 to 3, 4 to 6, 10 to 17). For typical expected fluctuating velocities and field strengths the normalized longitudinal tube wave energy fluxes F_L vary by roughly a factor of four around the value $2 \cdot 10^8\ erg\ cm^{-2} s^{-1}$.

In all cases displayed in Table 1, the time dependent wave computations were carried out for tube sections starting at the selected squeezing height and extending a few grid points higher. As we are presently interested only in the wave generation and not in the wave propagation or the physics of the tube, the length of the tube section was chosen to be small in order to save computation time. All calculations were extended to 5000 s. In our computations we assumed adiabatic conditions and did not consider shock formation. We found that for larger rms turbulent velocities u_t and for shallow squeezing heights the excitation produced rapid expansions of the computed tube section. This resulted in adiabatic cooling and eventually lead to unrealistically cold tubes with temperatures below 1000 K, where the wave computations broke down due to numerical difficulties. This occurred for $u_t \geq 2.1, 1.9, 1.9$ km/s at $\tau \leq 1, 10, 100$, respectively. We attribute this behaviour to our adiabatic treatment. In addition these upper limits of the excitation strength points to the limit of validity of the thin tube approximation employed by us.

Fig. 4 shows for case 2 of Table 1 (displayed also in Figs. 1 and 2) the time-dependence of the longitudinal tube wave flux together with the averaged wave flux. It is seen that the instantaneous wave flux is very stochastic in nature, consisting of intense

Table 1. Time-averaged longitudinal wave energy fluxes F_L (erg/cm^2s) generated in a tube of magnetic field strength B_0 (G), squeezed by velocity fluctuations at optical depth τ, with an rms turbulent velocity u_t (km/s). The fluxes are normalized to the solar surface at $\tau = 1$ by using an area factor A/A_0. Also shown are fitted flux values F_L^* using Eq. (27).

case	B_0	τ	A/A_0	u_t	F_L	F_L^*
1	1500	1	1.0	1.0	$1.1 \cdot 10^8$	$7.2 \cdot 10^7$
2	1500	10	.81	1.0	$7.4 \cdot 10^7$	$7.2 \cdot 10^7$
3	1500	100	.68	1.0	$6.8 \cdot 10^7$	$7.2 \cdot 10^7$
4	1500	1	1.0	1.7	$8.8 \cdot 10^8$	$6.5 \cdot 10^8$
5	1500	10	.81	1.7	$6.7 \cdot 10^8$	$6.5 \cdot 10^8$
6	1500	100	.68	1.7	$5.1 \cdot 10^8$	$6.5 \cdot 10^8$
7	1000	10	.81	1.0	$2.7 \cdot 10^8$	$2.6 \cdot 10^8$
8	1250	10	.81	1.0	$1.7 \cdot 10^8$	$1.3 \cdot 10^8$
9	1500	10	.81	1.0	$7.4 \cdot 10^7$	$7.2 \cdot 10^7$
10	1500	10	.81	0.9	$4.9 \cdot 10^7$	$4.7 \cdot 10^7$
11	1500	10	.81	1.1	$1.1 \cdot 10^8$	$1.1 \cdot 10^8$
12	1500	10	.81	1.3	$2.3 \cdot 10^8$	$2.1 \cdot 10^8$
13	1500	10	.81	1.5	$4.2 \cdot 10^8$	$3.9 \cdot 10^8$
14	1500	100	.68	0.9	$4.9 \cdot 10^7$	$4.7 \cdot 10^7$
15	1500	100	.68	1.1	$9.4 \cdot 10^7$	$1.1 \cdot 10^8$
16	1500	100	.68	1.3	$1.7 \cdot 10^8$	$2.1 \cdot 10^8$
17	1500	100	.68	1.5	$3.1 \cdot 10^8$	$3.9 \cdot 10^8$

short duration bursts. Comparison of Figs. 4 and 2 shows that the spikes in longitudinal wave flux are directly related to spikes in $v_{\|}$ and v_x. We recall that this behaviour is also seen in the transverse wave generation computations of Paper I.

The spectrum corresponding to this instantaneous wave energy flux is presented in Fig. 5, which again shows the stochastic nature of longitudinal tube wave generation. The spectra obtained for all other cases of Table 1 are similar to the one shown in Fig. 5. Thus, in order to compare spectra generated at different heights, with different squeezing velocities and different magnetic field strengths, we have to smooth them as otherwise no systematic trends can be seen. A standard smoothing procedure has been used for all cases. As a result of this smoothing, the low-frequency shape of the spectrum is preserved, however, the high-frequency tail seen in Fig. 5 is removed because its contribution to the total wave energy flux is negligible (see Fig. 4). Fig. 6 shows smoothed spectra of the longitudinal wave energy fluxes calculated for the tube $B_0 = 1500\ G$ and for the excitation at four different squeezing heights. It is seen that the smoothed wave energy spectra do not differ much with the excitation height for frequencies $\omega \approx 0.1\ Hz$. However, for higher frequencies, there is a tendency that squeezing at greater heights produces more wave energy. Even so, the total wave energy fluxes do not differ much, which is consistent with the time-integrated total fluxes given in Table 1.

The results presented in Fig. 7 clearly demonstrate that the shapes of the generated spectra are practically independent of the rms turbulent velocity u_t but its magnitude does strongly affect the total wave energy flux; the higher the velocity the more wave energy is generated. Moreover, the obtained results

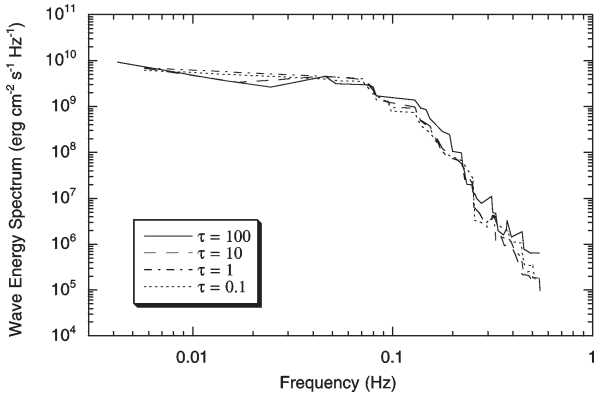

Fig. 6. Smoothed longitudinal tube wave energy spectra obtained for the excitation at different optical depths $\tau = 1, 10, 100$ and for a magnetic flux tube of the field strength $B = 1500\ G$ (cases 1 to 3 in Table 1). Also the case $\tau = 0.1$ is included for comparison. The spectra are shown as a function of circular frequency ω.

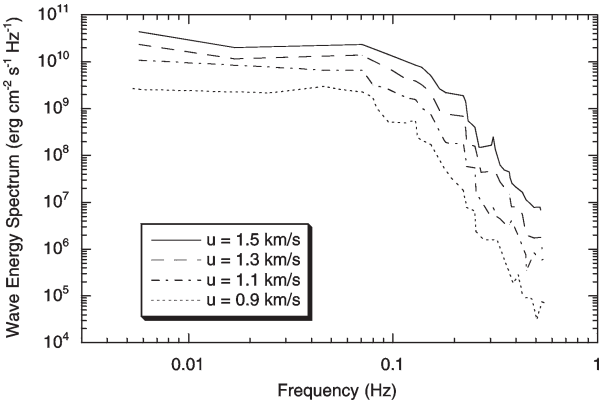

Fig. 7. Smoothed longitudinal tube wave energy spectra obtained for the excitation at the optical depth $\tau = 10$ with different rms turbulent velocities $u_t = 0.9, 1.1, 1.3, 1.5$, and for a magnetic flux tube of the field strength $B = 1500\ G$ (cases 10 to 13 in Table 1). The spectra are shown as a function of circular frequency ω.

also show that when the turbulent velocity increases, more wave energy is generated in the high-frequency domain of the spectra.

Finally, Fig. 8 shows the dependence of the wave energy spectrum on the flux tube model for the excitation at a common depth $\tau_{5000} = 10$. It is seen again that the shape of the spectra is practically independent of the strength of the magnetic field. However as noted above there is a significant dependence of the absolute wave flux on the field strength B_0.

The present results are now compared with our previous ones. Analytical calculations of the generation of linear longitudinal tube waves were performed by Musielak et al. (1989, 1995) who found that typical wave energy fluxes carried by these waves were of the order of $10^7\ erg/cm^2s$ (for $B_0 = 1500\ G$). Comparing the value $B_0 = 1500\ G$ with our results presented in Table 1, one sees that the nonlinear excitation of longitudinal tube waves gives fluxes typically more than one order of magnitude higher. This indicates that the linear results give only lower bounds for realistic wave energy fluxes carried by these waves

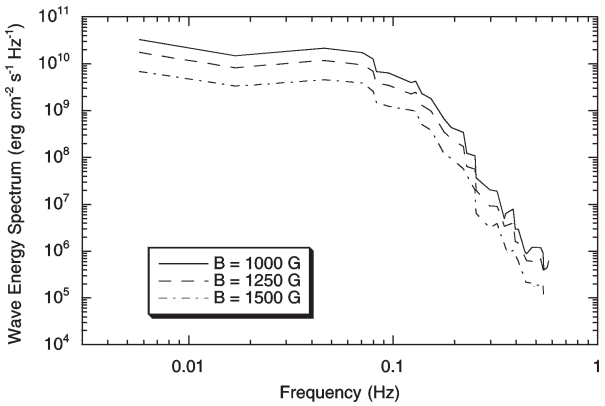

Fig. 8. Smoothed longitudinal tube wave energy spectra obtained for the excitation at the optical depth $\tau = 10$ and for flux tubes of different magnetic field strength $B = 1000, 1250, 1500\ G$ (cases 7, 8 and 9 in Table 1). The spectra are shown as a function of circular frequency ω.

in the solar atmosphere. As already mentioned in Paper I, the comparison must be taken with some caution because there is an important difference between the analytical and numerical approaches. Namely, in the numerical approach the process of squeezing or shaking a tube takes place only at one specific height, whereas in the analytical approach a significant portion of the entire flux tube is affected. Thus, the main difference is that the numerical approach does not take into account any correlation effects while the analytical approach does include some of them. It is presently unclear whether these correlation effects would decrease or increase the total wave energy fluxes.

Another difference between analytical and numerical results is the dependence of the wave generation process on the magnetic field strength. According to Musielak et al. (1995), the efficiency of the generation of linear longitudinal tube waves is strongly affected by the strength of the tube magnetic field; the stronger the field the lower is the resulting wave energy flux. The effect can be explained by the fact that "stiffness" of a flux tube decreases (and the gas pressure inside the tube increases) when the field strength decreases and, as a result, it is easier to squeeze the tube by external turbulent motions. Thus, for the same external motions, higher wave energy fluxes should be generated for weaker magnetic fields. Both our numerical and analytical results show this effect. While our analytical results (Musielak et al. 1995, Table 1) give $F_L \approx 2.8 \cdot 10^8, 1.1 \cdot 10^7\ erg\ cm^{-2} s^{-1}$ for the case of $\alpha = 1.5$, and $B_0 = 1000, 1500\ G$, respectively, we presently have $F_L \approx 2.7 \cdot 10^8, 7.4 \cdot 10^7\ erg\ cm^{-2} s^{-1}$, respectively for the same magnetic field strengths. This shows that for strong magnetic fields the difference between linear and nonlinear squeezing is particularly large.

Since the generated longitudinal tube waves are essentially acoustic waves guided by the magnetic field lines of a flux tube, it is also of interest to compare the tube wave fluxes with the acoustic wave fluxes outside the tube generated by the same turbulent motions in the solar convection zone. Recent calculations of the generation of linear acoustic waves performed by Musielak et al. (1994) showed that the total acoustic wave energy flux for the Sun is $1.7 \times 10^8\ erg/cm^2 s$ for the extended Kolmogorov energy spectrum with a modified Gaussian frequency factor, using a mixing length parameter of $\alpha = 2.0$. That this choice of mixing-length parameter is realistic, has recently been discussed by Theurer et al. (1997). Note that the turbulence spectrum for the acoustic case is the same which we employ in the present paper. Surprisingly it turns out that the value of the acoustic wave energy flux is roughly equal to the typical longitudinal tube wave flux found in our present work.

One might think that finding the same wave flux inside and outside the tube implies that the magnetic flux tube does not play a major role in the outer solar atmosphere, a result clearly in contradiction with the observations. The surprise quickly fades when one realizes that the gas density inside the tube is roughly a factor of 6 smaller than the external density. For this low density the wave flux in the tube is large compared to the outside flux, leading to rapid shock formation, but also to severe NLTE effects which strongly modify the radiative losses. To consider all these effects it is necessary to perform detailed calculations of the propagation and dissipation of these waves within magnetic flux tubes. Previous calculations by Herbold et al. (1985) for monochromatic waves and for a chosen range of wave energy fluxes showed that the waves formed shocks in the lower part of the chromosphere and heat the tube effectively. These results have been confirmed recently by Fawzy et al. (1998) who investigated the dissipation rates for waves of various energy fluxes in tubes of different geometry. In addition, Cuntz et al. (1998) adopted the approach presented here to calculate longitudinal wave energy fluxes for K2V stars with different rotation rates and used these results to construct the first purely theoretical models of stellar chromospheres for rotating stars.

Finally, the longitudinal wave energy fluxes must be compared with the transverse fluxes of Paper I. From our above revised typical transverse wave fluxes F_T we find a ratio $F_T/F_L \approx 30$. Estimates based directly on the observed velocities of the solar surface give similar magnitudes of the transverse wave energy fluxes (see Muller et al. 1994). These results have a simple physical explanation, namely, it is much easier to shake a magnetic flux tube by the external turbulent motions than to squeeze it. However, the dissipation rate for transverse waves is much lower than that for longitudinal waves. According to Ulmschneider et al. (1991), an efficient process of damping transverse waves is nonlinear coupling to longitudinal waves. This process may become active in the upper chromosphere after the propagating transverse waves reach large enough amplitudes. Thus, one may conclude that the upper chromospheric layers are heated by these waves, whereas longitudinal waves are responsible for the heating of the lower chromospheric layers. In the following, we show that this simplified picture has to be taken with caution.

Since the described calculations are limited to the thin flux tube approximation, a number of important physical processes that may strongly influence the energy propagation along the magnetic tubes are not considered. Aside of the appearance of compressive 'sloshing modes' the dissipation properties of which have not been investigated, there is wave energy leakage

from flux tubes to the external medium (Ziegler & Ulmschneider 1997a). Another process is the generation of wave energy from external acoustic waves. To get some idea about the efficiency of the latter processes, we refer to 2-D time-dependent MHD wave simulations performed by Huang (1996). The obtained results for magnetic slabs with $\beta < 1$ showed that almost 60% of the energy carried by transverse waves and 30% of the energy carried by longitudinal waves can leak out to the external medium within two wave periods. In addition, Huang showed that the generation of wave energy in the magnetic slabs of the same β by external acoustic waves is only about 15% for both wave modes. This makes the net leakage for transverse waves significant but practically allows to neglect the net leakage for longitudinal waves. The results of 3D time-dependent MHD simulations of magnetic flux tubes performed by Ziegler & Ulmschneider (1997b) showed that the leakage for transverse waves can be even higher. This means that these waves will contribute energy to the external acoustic wave field, but given the small filling factors of magnetic tubes outside the inner network, this transverse energy will not enhance much the outside acoustic flux.

4. Conclusions

From our studies of nonlinear generation of longitudinal waves in solar magnetic flux tubes excited by the external turbulent velocities at various heights, the following conclusions can be drawn.

1. The time-averaged longitudinal wave energy fluxes $\overline{F}$ calculated for a single magnetic flux tube embedded in the solar atmosphere are of the order $2 \cdot 10^8\ erg\ cm^{-2}s^{-1}$, which is roughly equal to the pure acoustic flux outside the tube. The calculated spectrum for longitudinal tube waves is broadly similar to that of the exciting turbulent velocity, namely, it is relatively constant at low frequencies and decreases rapidly for frequencies higher than $\omega = 0.1\ Hz$.

2. The longitudinal wave energy spectra and the corresponding fluxes do not vary much with the height where the tube is squeezed. For large rms turbulent velocities ($u_t \geq 1.9$) km/s, the calculations stopped because rapid tube expansion led to very low tube temperatures ($T < 1000$) K.

3. The shape of the calculated wave energy spectra remains practically unchanged when the squeezing velocity is increased, but the longitudinal wave energy fluxes increase with the rms turbulent velocity u_t like $F_L \sim u_t^4$.

4. Increasing the magnetic field strength in the tube does not change the shape of the wave energy spectrum, but increasing the field strength from $B_0 = 1000\ G$ to $1500\ G$, decreases the longitudinal wave flux by a factor of 3.6. It is found that $F_L \sim B_0^{-3}$.

5. The transverse wave fluxes of Huang et al. (1995) have to be revised upwards to values of the order of $6.0 \cdot 10^9\ erg\ cm^{-2}s^{-1}$, due to an error and by considering two orthogonal horizontal shaking directions. This is roughly similar to the fluxes estimated from observations of the proper motion of network bright points (Muller et al. 1994).

6. The obtained longitudinal wave energy fluxes are up to one order of magnitude higher than those found by using analytical methods (Musielak et al. 1995), but they are about a factor of 30 lower than the transverse wave fluxes. For the latter severe leakage out of the tube may occur.

There are several reasons that our approach has to be considered as idealized and simplified. First, the squeezing takes place only at a local height point and does not include the correlation effects which occur when the tube is squeezed over its entire length. Second, reflection and wave energy losses through nonlinear wave coupling, leakage, shock formation and atmospheric damping are not taken into account.

Acknowledgements. This work was supported by the NASA Astrophysics Theory Program under grant NAG5-3027 (Z.E.M. and P.U.), by NASA/MSFC under grant NAG8-839 (Z.E.M.), by NSF under grant ATM-9526196 (Z.E.M.), and by NATO under grant CRG-910058 (P.U. and Z.E.M.). Z.E.M. also acknowledges the support of this work by the Alexander von Humboldt Foundation. The authors thank W. Rammacher for help with the numerical code and S.R.O. Ploner for help with the manuscript.

References

Bohn H.U., 1981, Ph.D. Thesis, Univ. Würzburg, Germany
Bohn H.U., 1984, A&A 136, 338
Cattaneo F., Brummell N.H., Toomre J., Malagoli A., Hulburt, N.E., 1991, ApJ 370, 282
Cheng J., 1992, A&A 264, 243
Choudhuri A.R., Auffret H., Priest E.R., 1993a, Sol. Phys. 143, 49
Choudhuri A.R., Dikpati M., Banerjee D., 1993b, ApJ 413, 811
Cuntz M., Ulmschneider P., Musielak Z. E., 1998, ApJ 493, L117
Defouw R.J., 1976, ApJ 209, 266
Fawzy D., Ulmschneider P., Cuntz M., 1998, A&A in press
Goldreich P., & Kumar P., 1988, ApJ 326, 462
Goldreich P., & Kumar P., 1990, ApJ 363, 694
Hasan S.S., 1997, ApJ 480, 803
Herbold G., Ulmschneider P., Spruit H.C., Rosner R., 1985, A&A 145, 157
Huang P., 1996, Phys. Plasmas 3, 2579
Huang P., Musielak, Z.E., Ulmschneider P., 1995, A&A 279, 579 (Paper I)
Landau L.D., Lifshitz E.M., 1959, Fluid Mechanics, Pergamon Press, London
Moreno-Insertis F., Schüssler M., Ferriz-Mas A., 1997, A&A 312, 317
Muller R., 1989, in: Solar and Stellar Granulation, R.J. Rutten & G. Severino, Eds., Kluwer Academic Publ., Dordrecht, p. 101
Muller R., Roudier Th., Vigneau J., Auffret H., 1994, A&A 283, 232
Musielak Z.E., Rosner R., Ulmschneider P., 1989, ApJ 337, 470
Musielak Z.E., Rosner R., Gail H. P., Ulmschneider P., 1995, ApJ 448, 865
Musielak Z.E., Rosner R., Stein, R.F., Ulmschneider P., 1994, ApJ 423, 474
Narain U., Ulmschneider P., 1996, Space Sci Rev. 75, 453
Nesis, A. et al., 1992, ApJ, 399, L99
Nordlund A., Dravins D., 1990, A&A 238, 155
Nordlund A., Spruit H.C., Ludwig H.-G., Trampedach R., 1997, A&A 328, 229
Nordlund A., Stein R.F., 1991, in: Stellar Atmospheres: Beyond Classical Models, L. Crivellari & I. Hubeny, Eds., NATO ASI Series, Kluwer Academic Publ., Dordrecht, p. 263

Ossin A., Volin S., Ulmschneider P., 1998, A&A in press
Roberts B., Webb A.R., 1979, Solar Phys. 64, 77
Solanki S.K., Rüedi I., Bianda M., Steffen M., 1996a, A&A 308, 623
Solanki S.K., Zufferey D., Lin H., et al., 1996b, A&A 310, L33
Spruit H.C., 1981, A&A 98, 155
Steffen M., 1993 , Habil. Thesis, Univ. Kiel, Germany
Steffen M., Freytag B., Holweger H.: 1994, in: Solar Magnetic Fields, M. Schüssler & W. Schmidt, Eds., Cambridge Univ. Press, Cambridge, p. 298
Stein R.F., 1967, Sol. Phys. 2, 385
Steiner O., Grossmann-Doerth, Schüssler, M., Knölker M., 1996, Sol. Phys. 164, 223
Steiner O., Grossmann-Doerth, Knölker M., Schüssler, M., 1998, ApJ 495, 468
Theurer J., Ulmschneider P., Kalkofen W., 1997, A&A 324, 717
Ulmschneider P., Zähringer K., Musielak Z.E., 1991, A&A 241, 625
Vernazza J.E., Avrett E.H., Loeser R., 1981, ApJ Suppl. 45, 635
Zahn J.-P., 1987, Lecture Notes in Physics, 292, Solar and Stellar Physics, Eds. E.H. Schröter & M. Schüssler (Berlin: Springer-Verlag), 55
Zhugzhda Y., Bromm V., Ulmschneider P., 1995, A&A 300, 302
Ziegler U., Ulmschneider P. 1997a, A&A 324, 417
Ziegler U., Ulmschneider P. 1997b, A&A 327, 854